minerals

MDPI

Article

# Optimisation of a Multi-Gravity Separator with Novel Modifications for the Recovery of Ferberite

**Robert Fitzpatrick [1,*], Patrick Hegarty [1], Keith Fergusson [1], Gavyn Rollinson [1], Weiguo Xie [1] and Treve Mildren [2]**

[1] Camborne School of Mines, University of Exeter, Penryn Campus, Exeter TR10 9FE, UK; P.B.Hegarty@exeter.ac.uk (P.H.); keith.fergusson@live.com (K.F.); G.K.Rollinson@exeter.ac.uk (G.R.); W.Xie@exeter.ac.uk (W.X.)

[2] Gravity Mining Ltd., Glencarrow, New Road, Stithians TR3 7BL, UK; treve@gravitymining.com

* Correspondence: R.S.Fitzpatrick@exeter.ac.uk; Tel.: +44-(0)1326-254-141

Received: 15 February 2018; Accepted: 20 April 2018; Published: 2 May 2018


**Abstract:** Tungsten is considered by the European Union as a critical raw material for future development due to its expected demand and scarcity of resource within Europe. It is therefore, critical to optimize European tungsten operations and maximise recoveries. The role of enhanced gravity/centrifugal concentrators in recovering tungsten from ultra-fine fractions should form an important part of this aim. Reported herein are the results of investigations to improve efficiency of Wolf Minerals' Draklends mine, a major European tungsten mine, by recovering saleable material from a magnetic waste stream of a low-intensity magnetic separator using an enhanced gravity concentrator. The mine hosts wolframite and ferberite as the main tungsten bearing mineral species. A Mozley multi-gravity separator (MGS) C-900 was selected as it is suited to exploiting small variations in mineral density to affect a separation. Working with a current manufacturer, a novel scraping blade system was tested. To assess the MGS in a statistically valid manner, a response surface methodology was followed to determine optimal test conditions. The test programme showed that the most important parameters were drum speed and wash water rate. Under optimal conditions the model predicted that 40% of the tungsten could be recovered above the required grade of 43% $WO_3$.

**Keywords:** centrifugal gravity separation; tungsten-bearing minerals; quantitative mineralogy; response surface method; central composite rotatable design

## 1. Introduction

### 1.1. Background

Tungsten is recognised by the European Union as one of 27 critical raw materials for future economic growth and prosperity. Tungsten has a wide range of properties due to its unique physical properties which include extremely high melting point and hardness when alloyed with carbon. The principle application of tungsten is as a cemented carbide followed by alloys with various other metals. This economic importance combined with a high reliance on imports into the EU, have led to the classification as a critical metal, see Figure 1.

The European Union imported 15,000 tonnes of tungsten concentrate in 2012, relying on Russia for 98% of the total. World supply of tungsten is dominated by China which in 2012 produced 85% of global supply and consumed 51% [2]. To help reduce the reliance on import of tungsten the European Union has providing funding for the OptimOre project (Horizon 2020 research and innovation programme grant 642201). One objective of this project is to optimise the processing of tungsten ores to help diversify global supply and make European deposits more competitive. To support this objective

this article reports the results of using an enhanced gravity concentrator to improve the recovery of tungsten at the Drakelands mine, a major European mine site operated by Wolf Minerals Ltd. Specifically, investigations were undertaken to optimise recovery of tungsten-bearing minerals using a Mozley MGS with novel modifications. The objective of the work was to assess the feasibility of producing a saleable product from this stream and to compare the novel modifications to the MGS with the conventional system.

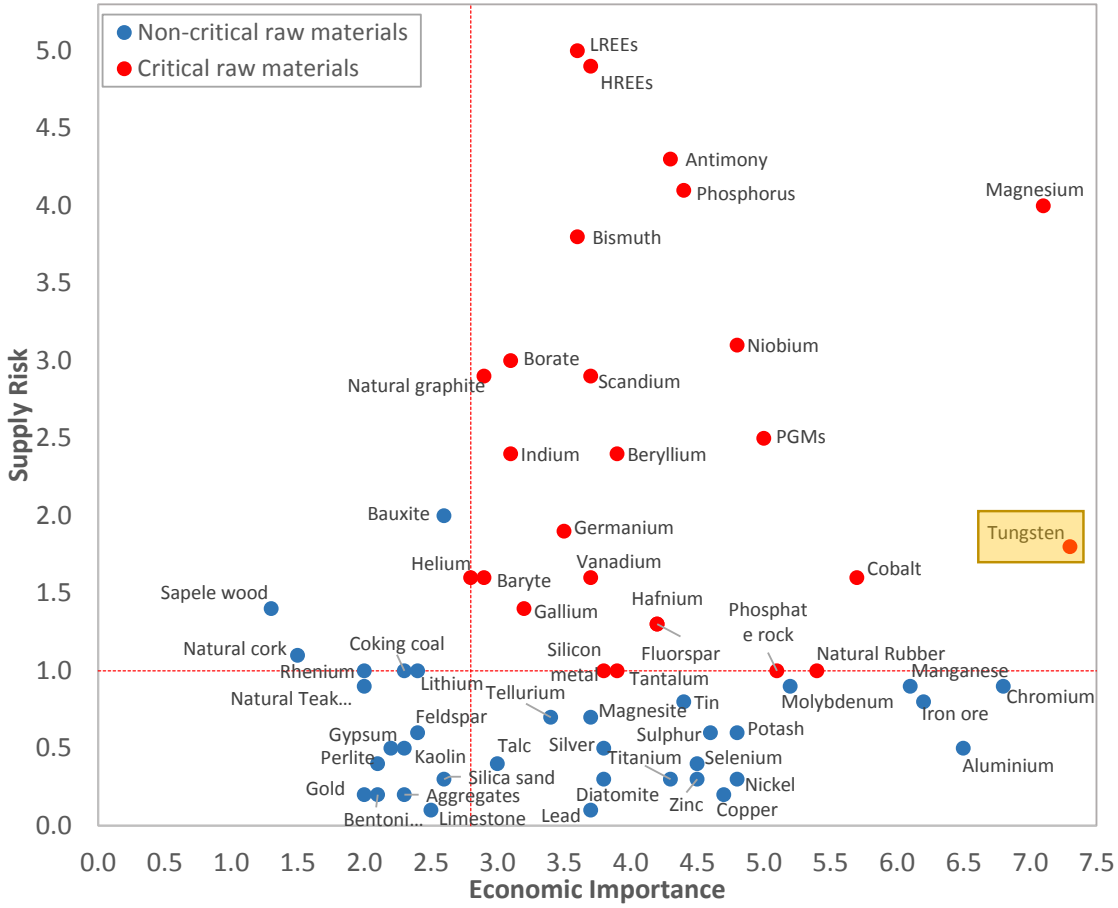


**Figure 1.** European Commission criticality assessment for raw materials with critical materials highlighted in red, tungsten has been further highlighted by the authors [1].

The feed to the LIMS separator is gravity concentrate which has been roasted under reducing conditions to convert hematite ($Fe_2O_3$) to magnetite ($Fe_3O_4$). The LIMS magnetic stream is currently treated as waste but has a high tungsten grade (over 20%) and so represents a measurable loss within the operation. If saleable material can be recovered from this stream in an efficient manner it will increase profitability at the mine site and help to decrease the energy per tonne of concentrate produced. Both of these outcomes are important to help ensure the competitiveness of European based mines in a global market dominated by a small number of countries.

### *1.2. Multi-Gravity Separator Device*

The multi-gravity separator (MGS) also known as the enhanced-gravity separator (EGS) was designed in the late 1980's to early 1990's for the concentration of fine and ultra-fine heavy minerals, with early applications focusing on cassiterite, chromite, celestite and magnetite [3]. The machine operates on similar principles to a shaking table but utilises rotational motion to generate centrifugal forces greater than those of gravity. This increase in force allows for more efficient separation at finer

sizes. The main design and operating variables of the MGS are summarised in Figure 2 alongside the principle forces acting on a particle.

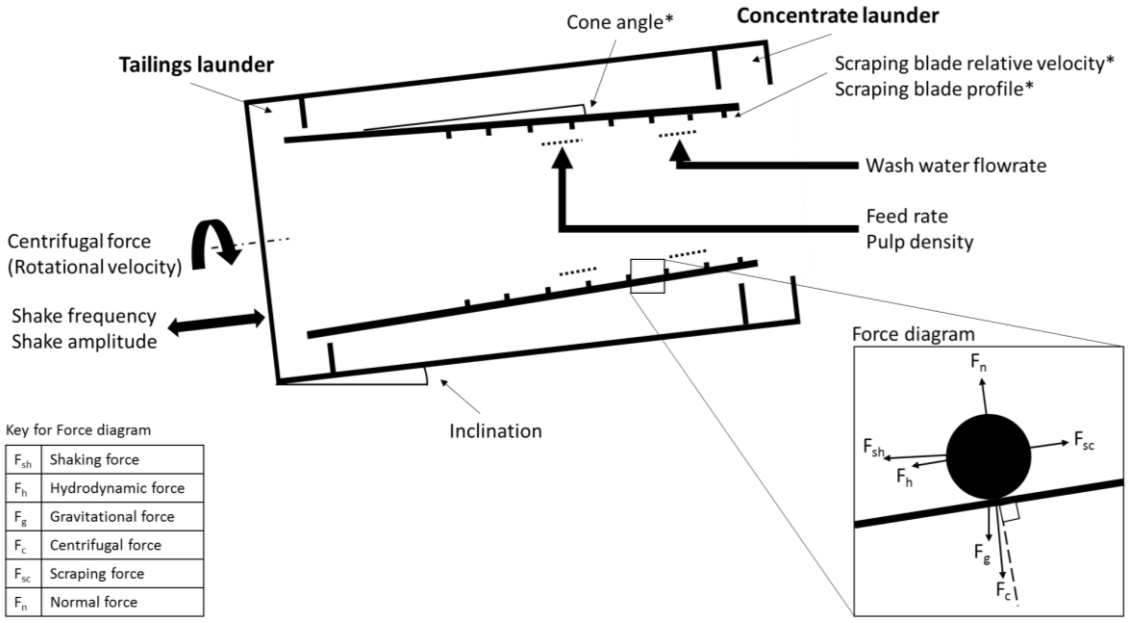


**Figure 2.** MGS operating and design (denoted with *) variables and principle forces (Force Diagram modified after [4]).

Due to the large number of variables and interactions, most modelling work for the MGS has consisted of determining optimal conditions using regression analysis. A review of this research literature reveals that the rotational velocity of the drum has been identified as the most important factor on grade and recovery [5–8].

Both [5,7] concluded that rotational velocity and pulp density were the most important factors with regards to optimisation. In [6] the conclusion was that rotational velocity had a significant impact whereas inclination and wash water flowrate had a trivial effect on performance. In [8] it was observed that wash water had an important interaction with performance at high wash water flowrates and high rotational velocity. The authors of [5] also observed an important interaction between wash water and pulp density.

To quantify the results reported in literature, a boxplot was constructed to illustrate the relative importance of operating variables on grade and recovery when using a Mozley MGS (Figure 3). It was constructed by analysing the results published in six research articles ([5,8–12]).

The level of influence for each variable was judged using the relative change in the adjusted $R^2$ measure of model fit when a variable was removed.

Figure 3 shows that the rotational velocity is the most important operating variable for the performance of the MGS. Shake amplitude was found to have a wide variation in importance. All the research articles used inclination as a variable factor though it's influence on performance appears relatively small. There was only one paper which investigated the effect of the pulp density (% solids) on MGS performance and it was found to have a significant influence on performance.

Although a good deal has been reported on the effect of operating variables on MGS performance much less attention has been paid to design variables. The author could find no published research on the influence of changes to design variables on MGS performance. The cone angle, the shape or profile of scraping blades and the relative velocity between drum and scraping blade would all be expected to have an influence on performance but have not been properly investigated. It was noted in [4] that it was 'odd' that the relative velocity of blades had not previously been investigated as the force of the blades ($F_{SC}$) is the only one acting in the direction of the concentrate outlet (see force diagram in

Figure 2). It can be further stated that the profile of the scraping blade will also have an important effect on the force directed towards the concentrate outlet.

A new scraping blade design has been developed by Gravity Mining Ltd. (Cornwall, UK) and fitted to a Mozley C-900 MGS unit located at the Camborne School of Mines, University of Exeter, UK. The scraping blades are low profile in comparison to the traditional blades. In theory, less dense particles not pinned to the drum will weir over the blades so that only the densest material is carried to the concentrate outlet. Photos of the fitted scraping blade systems are shown in Figure 4 whilst schematics demonstrating their theoretical operating principle is shown in Figures 5 and 6.

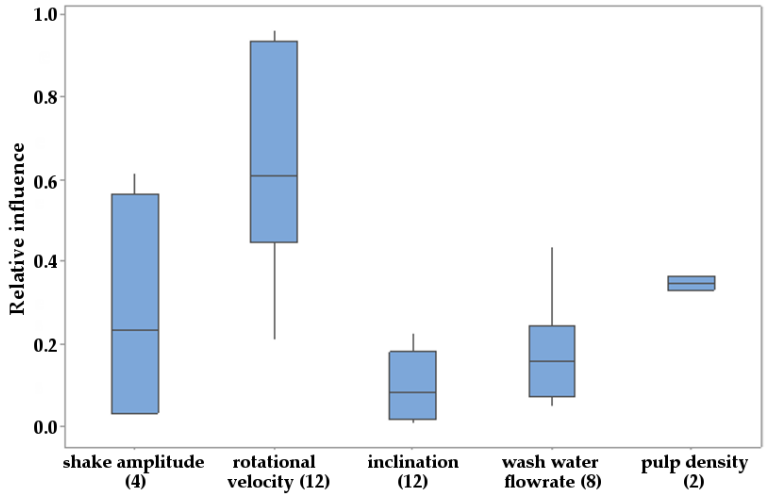


**Figure 3.** Boxplot of relative importance of operational variables on grade and recovery based on relative change in the adjusted $R^2$ measure of model fit on removing a variable. Brackets indicate number of data points.

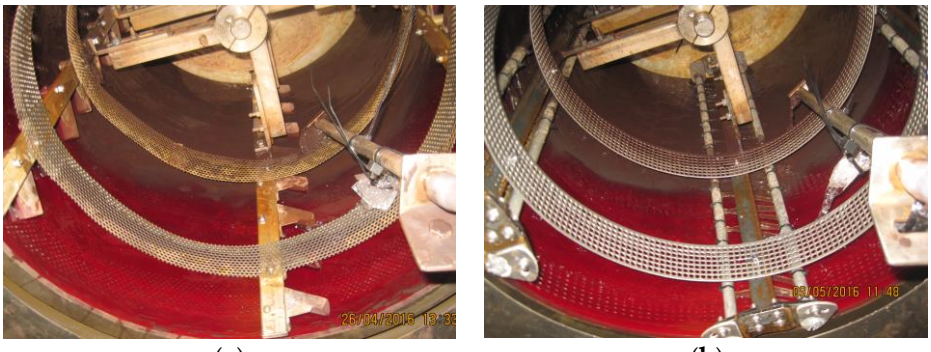


**Figure 4.** (**a**) Photograph of Mozley C-900 MGS with conventional scraping blades; (**b**) photograph of Mozley C-900 MGS with novel, low profile scraping blades.

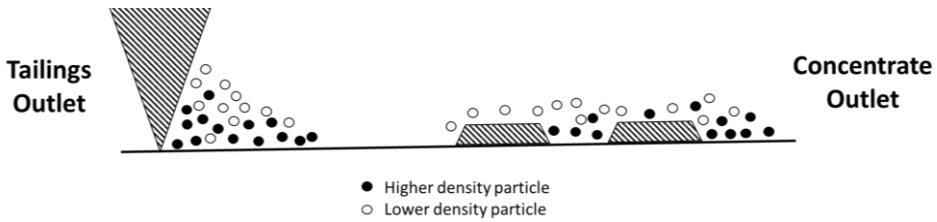


**Figure 5.** Cross-sectional view of scraping blades. Conventional scraping blade system is shown on the left and the novel, low profile scraping blades on the right.

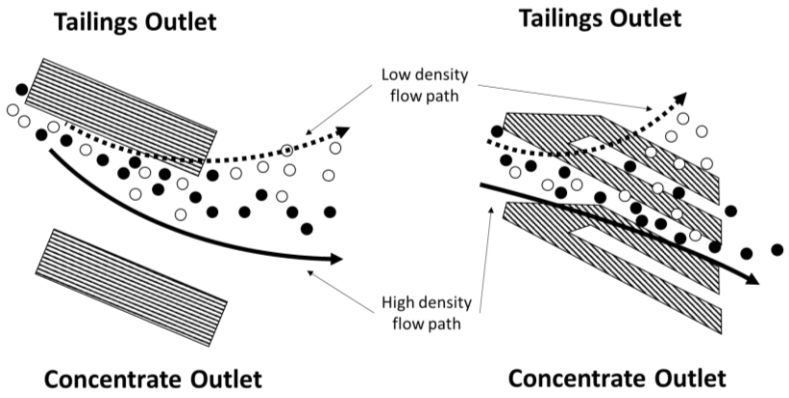


**Figure 6.** Plan view of scraping blades. Conventional scraping blade system is shown on the left and the novel, low profile scraping blades on the right.

## 2. Materials and Methods

### *2.1. Ore Sample*

Approximately 25 kg of material was collected in early 2016 from the magnetic product stream from a low intensity magnetic separator used in the processing plant of Drakelands mine. This material had a grade of about 23% $WO_3$ and the minimum acceptable grade for blending is 43% $WO_3$ which indicated that the LIMS magnetic stream was a waste fraction but only a modest upgrading would be required to produce a saleable product. This would increase plant recovery and potentially reduce energy input per tonne of concentrate produced. Gravity separation was an attractive option to process this material as the plant is already familiar with the technology and gravity separation represents a low capital cots, low energy and low environmental impact solution in comparison to alternative techniques such as froth flotation.

Prior knowledge of the plant, indicated that the material would likely contain ferberite (S.G. 7.45) as the principle ore mineral and reduced hematite/magnetite (S.G. 5.1–5.3) as the principle gangue mineral. As the ore and gangue minerals are expected to have similar densities the separation would be expected to be difficult. The MGS is suited to exploiting small variations in mineral density to affect a separation. For example, the MGS has been used historically for the separation of chromite from goethite [3].

Based on the above, the material is a useful test material as it is a good example of material which is difficult to recover using conventional approaches and is suited to the MGS. The testwork described herein was undertaken with the aim of optimising the separation of this material and further, to test whether the novel scrapping blades improve performance for this material.

From the as received sample, representative sub-samples were collected for chemical and mineralogical analyses. The remaining material was stage-ground using a stainless-steel batch rod mill until 100% of the material passed through a 90 μm aperture sieve. This size range is suited to the MGS which operates most effectively on fine material with optimum performance suggested to occur at less than 53 μm [13]. This size range also made material handling and pumping more practical. Size analysis of the ground material was completed using a Malvern MasterSizer 3000 (Malvern Panalytical Ltd., Malvern, UK), a laser diffraction particle analyser.

### *2.2. Chemical and Mineralogical Analysis*

All chemical and mineralogical analyses were undertaken in the Camborne School of Mines chemical and imaging mineralogical facility, Penryn, UK. Bulk geochemical analysis was carried out using an Olympus DP-6000C portable XRF analyser (Olympus UK & Ireland, Southend-on-sea, UK with calibration using a Bruker S4 Pioneer WDS X-ray Fluorescence (XRF) instrument (Bruker AXS Ltd., Coventry, UK).

Quantitative mineralogical analysis was conducted using a QEMSCAN® 4300 (Thermo-Fisher, formally FEI Company, Eindhoven, The Netherlands) which is based on a Zeiss EVO 50 series SEM and consists of four light elements Bruker SDD (Silicon Drift Droplet) Energy Dispersive X-ray Spectrometers (EDS) and an electron backscatter detector. Samples were prepared as resin blocks impregnated with carbon to minimize settling. The whole sample block was analysed in fieldscan measurement mode with 10 µm X-ray spacing, then granulated into 11,848 particles. The software iMeasure v. 4.2 was used for data acquisition, and iDiscover v. 4.2 and 4.3 were used for the data processing. Further manipulation of the QEMSCAN data was undertaken using Mathworks Matlab 2017b (MathWorks, Natick, MA, USA).

Electron microprobe analysis was completed using a JEOL JXA-8200 microprobe (Joel USA Inc., Peabody, MA, USA) using a 15 nA electron beam with a probe current of $3.1 \times 10^{-8}$ accelerated to 15 kV and focused to a 5 µm beam diameter using wavelength dispersive X-ray spectrometers only. The microprobe was calibrated to five elements using a ZAF matrix correction routine. The elements analysed were bismuth, tungsten, tin, iron and manganese measured at 87 points identified as ferberite by QEMSCAN.

### *2.3. Experimental Approach for Selective Concentration by Enhanced Gravity Separator*

To test the effectiveness of the new scraping blade system a series of tests were undertaken in the Mozley C-900 MGS modified to include the new blades. Three operating variables were selected based on the review of previous studies to optimise the separation of LIMS waste material with the new blades. These were the rotational velocity, wash water flowrate and pulp density. All other operating variables were maintained at constant levels throughout the experimental program.

Initial tests were completed to determine the length of time required to reach a steady state with regards to mass pull, grade and recovery during an experimental run. To investigate the effect of this procedure on the separation and the effects of further changes to wash water flowrate, samples were collected at regular intervals from the beginning of an experimental run and after a further change in flowrate.

Screening experiments were undertaken with the LIMS waste material to determine suitable ranges for the operating variables. The screening experiments indicated that only a small range of rotational velocities was suitable. It was not possible to recover any concentrate under the most favourable conditions with velocities less than 130 RPM and above 150 RPM it was not possible to upgrade the material as hematite was recovered as well as ferberite. It was found that slurries with less than 30% solids by mass would not produce a concentrate product under high levels of wash water. Based on these screening experiments, the ranges chosen for the experiment were 130 to 150 RPM, 2 to 7 L per minute wash water and pulp density of 25% to 45% solids.

A set of experiments informed by a Central Composite Rotatable Design (CCRD) was then undertaken using the Response Surface Methodology (RSM) to create a model for the processing of the LIMS waste material through a MGS C-900 with new blades. The three operating variables selected were varied according to the experimental design whilst all other operating variables were maintained at constant levels throughout the experimental program. This approach was selected as it has been shown to be beneficial for optimisation for the MGS [6,9] as well as other gravity separation and mineral processing equipment [14].

The CCRD is based on a 2 level factorial design with its origin at the centre and additional axial points, β, at set distances from the centre. Repeat runs were undertaken at the central point to estimate experimental error. The axial points were determined with the use of Equation (1) and the number of test runs required is determined by Equation (2) where $k$ is the number of factors and $n_0$ the number of centre point runs [15]. Six centre point runs were selected for this model which was processed using the statistical analysis software, Minitab 17.

$$\alpha = 2^{k/4} \quad (1)$$

$$\text{number of runs} = 2^k + 2 \cdot k + n_0 \quad (2)$$

Based on (1) and (2) the value of $\alpha$ is 1.682 ($2^{3/4}$) and the number of runs is 20 ($2^3$ + 2·3 + 6). The variable levels used are summarised in Table 1, whilst the full experimental design is shown in Table 2. The order of the experiments was randomised before testing.

**Table 1.** Summary of values used for variable levels in CCRD experimental design programme.

| | Coded Variable Value | | | | |
|---|---|---|---|---|---|
| | $-\beta$ | $-1$ | 0 | $+1$ | $+\beta$ |
| | $x_{n,min}$ | $\left(\frac{x_{n,max}+x_{n,min}}{2}\right) - \left(\frac{x_{n,max}-x_{n,min}}{2\alpha}\right)$ | $\left(\frac{x_{n,max}+x_{n,min}}{2}\right)$ | $\left(\frac{x_{n,max}+x_{n,min}}{2}\right) + \left(\frac{x_{n,max}-x_{n,min}}{2\alpha}\right)$ | $x_{n,max}$ |
| Rotational velocity, rpm ($x_1$) | 130 | 134.1 | 140 | 145.9 | 150 |
| Wash water flowrate, lpm ($x_2$) | 2 | 3 | 4.5 | 6 | 7 |
| Pulp density, % solids ($x_3$) | 25 | 29.1 | 35 | 40.9 | 45 |

**Table 2.** Summary of experimental runs in CCRD experimental design programme.

| Std Order | Coded | | | Uncoded | | |
|---|---|---|---|---|---|---|
| | $x_1$ | $x_2$ | $x_3$ | Rotational Velocity, rpm | Wash Water Flowarate, lpm | Pulp Density, % Solids |
| 1 | −1 | −1 | −1 | 134.1 | 3 | 29.1 |
| 2 | 1 | −1 | −1 | 145.9 | 3 | 29.1 |
| 3 | −1 | 1 | −1 | 134.1 | 6 | 29.1 |
| 4 | 1 | 1 | −1 | 145.9 | 6 | 29.1 |
| 5 | −1 | −1 | 1 | 134.1 | 3 | 40.9 |
| 6 | 1 | −1 | 1 | 145.9 | 3 | 40.9 |
| 7 | −1 | 1 | 1 | 134.1 | 6 | 40.9 |
| 8 | 1 | 1 | 1 | 145.9 | 6 | 40.9 |
| 9 | $-\beta$ | 0 | 0 | 130.1 | 4.5 | 35 |
| 10 | $+\beta$ | 0 | 0 | 149.9 | 4.5 | 35 |
| 11 | 0 | $-\beta$ | 0 | 140 | 2 | 35 |
| 12 | 0 | $+\beta$ | 0 | 140 | 7 | 35 |
| 13 | 0 | 0 | $-\beta$ | 140 | 4.5 | 25.1 |
| 14 | 0 | 0 | $+\beta$ | 140 | 4.5 | 44.9 |
| 15 | 0 | 0 | 0 | 140 | 4.5 | 35 |
| 16 | 0 | 0 | 0 | 140 | 4.5 | 35 |
| 17 | 0 | 0 | 0 | 140 | 4.5 | 35 |
| 18 | 0 | 0 | 0 | 140 | 4.5 | 35 |
| 19 | 0 | 0 | 0 | 140 | 4.5 | 35 |
| 20 | 0 | 0 | 0 | 140 | 4.5 | 35 |

Due to the relatively low mass of material it was necessary to recycle the 25 kg sample between experimental test runs. To minimise loss of fines, test products were left to settle for a minimum of 4 h before decantation and preparation of feed slurries. Some of the decanted water was then added to create the required pulp density for the next test run. The feed grade was monitored during the test programme to assess loss of ferberite which is known to be friable and most likely to breakdown during experimentation and accumulate in the finer fractions. Any decrease in feed grade during testing could affect the reliability of trends in the results.

Tests using conventional scraping blades were undertaken both before the CCRD experimental design programme and afterwards. This was done to minimise any bias resulting from deterioration of material or loss of fines. These tests were undertaken using the same methodology as during the CCRD programme.

## 3. Results and Discussion

### *3.1. Sample Characterisation by Chemical and Mineralogcial Analysis*

The Chemical composition of the elements of interest in the LIMS magnetic fraction are summarised in Table 3.

Table 3 shows that the major elements within the LIMS magnetic waste stream are tungsten and iron which is expected given that the material is the magnetic fraction of a gravity pre-concentrate. The values obtained by QEMSCAN agree well with the results obtained by XRF which is good evidence that the QEMSCAN sample was suitably representative.

Mineralogical analysis of the LIMS magnetic waste material was undertaken to better understand the composition and better qualify the appropriateness of using an MGS for separation. A summary of the modal mineralogy reported by QEMSCAN analysis is shown in Figure 7.

**Table 3.** Distribution of elements of interest in the LIMS magnetic waste material as measured by XRF and QEMSCAN.

| Analysis Type | $WO_3$ | $Fe_3$ | Mn | $Sn_2$ | $Si_2$ |
|---|---|---|---|---|---|
| XRF | 22.95 | 53.09 | 0.72 | 1.33 | 0.18 |
| QEMSCAN | 20.45 | 49.71 | 0.39 | 0.15 | 0.34 |

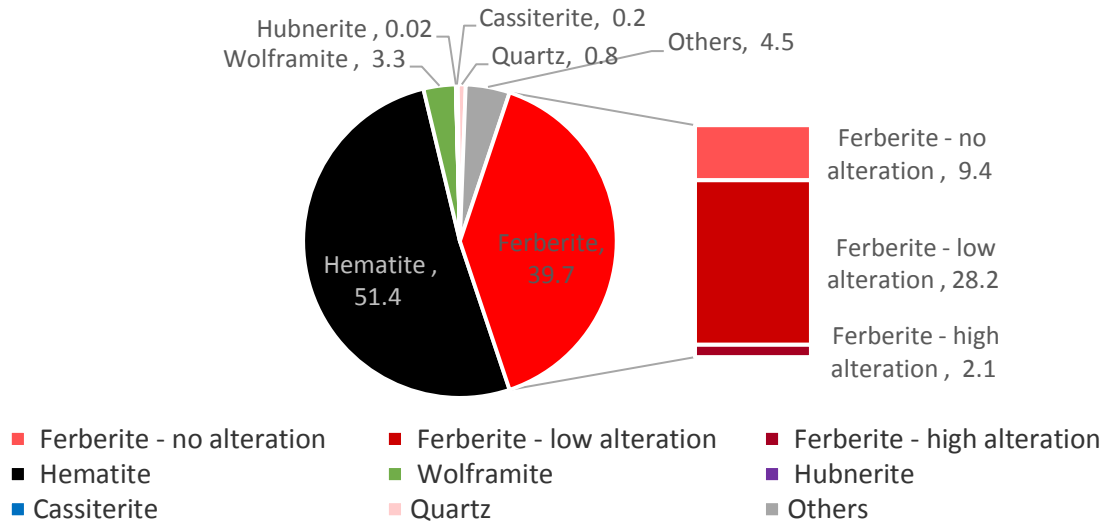


**Figure 7.** Summary of modal mineralogy of LIMS waste stream material based on QEMSCAN analysis.

The data in Figure 7 agrees with prior knowledge of the material. It shows that the LIMS magnetic waste material contains 43.1% tungsten-bearing minerals by mass and that ferberite is the dominant tungsten-bearing species accounting for 92% of these minerals. As expected, the other major mineral present is hematite which accounts for 51.4% of the mass. Combined, the tungsten-bearing minerals and hematite account for 94.5% of the sample mass. The QEMSCAN analyses showed that the chemistry of ferberite grains was varied because of weathering. Specifically, the ferberite showed signs of hematisation which is the replacement of tungsten by iron in the grain. This was accounted for in QEMSCAN by dividing ferberite arbitrarily into three categories based on the degree of hematisation as indicated by EDS chemistry (Figure 7). The majority of the ferberite in the LIMS waste stream (75%) is weathered with a relatively low level of alteration. Approximately 5% is highly weathered and altered. The extent of hematisation was further quantified using EPMA. The results of these analyses are summarised in Figure 8.

Figure 8 shows the relative molar proportions of W, Fe and Mn for the three sub-categories of ferberite. It can be seen that the tungsten content varies from the theoretical maximum of 50% or 1:1 molar ratio of W:(Fe,Mn) to a pseudo-hematite containing less than 5% tungsten. There is evidence in Figure 8 that data points with high manganese content generally have little tungsten depletion (circled points in Figure 8). It would be expected that this identified trend would continue if particles classified by QEMSCAN as wolframite and hubnerite were also analysed by EPMA. This observation is

in line with the theory that the wolframite is not directly weathered but first undergoes ferberitisation before hematisation, i.e., replacement of tungsten with iron [16]. Hematisation of the ferberite and the resultant variation in tungsten to iron ratios will affect the specific gravity of particles. This problem is compounded by cavitation and an increased porosity which further reduces the specific gravity due to trapped gangue minerals air. The depletion of tungsten combined with added buoyancy is problematic for gravity separation as the specific density is linked to these factors. The expected recovery using physical separation is also limited as some of the tungsten bearing mineral grains fall below the required grade for blending.

Having established that variations in the density of tungsten bearing minerals were expected, to better understand the feasibility of separating these minerals the mineral liberations and associations were analysed. The tungsten-bearing minerals are well liberated with 93.2% of particles being at least 90% liberated. There is only a 20% association between ferberite and hematite as shown in Table 4.

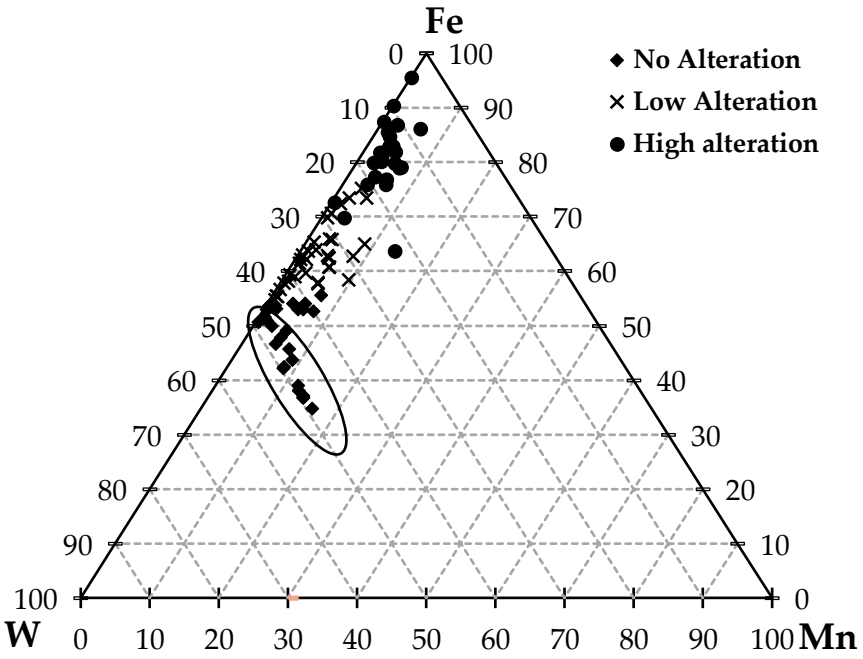


**Figure 8.** Ternary plot from EPMA analysis of points identified as ferberite by QEMSCAN. The circled region highlights points with relatively high manganese content which show little tungsten depletion.

**Table 4.** Mineral associations within the LIMS waste stream sample as reported by QEMSCAN, each column totals to 100% association.

| | Background | Wolframite | Ferberite | Hubnerite | Cassiterite | Fe Oxide | Quartz |
|---|---|---|---|---|---|---|---|
| **Background** | 0.00 | 8.3 | 47.1 | 4.1 | 24.3 | 59.5 | 32.3 |
| **Wolframite** | 1.5 | 0.0 | 27.2 | 73.0 | 3.3 | 0.5 | 1.0 |
| **Ferberite** | 27.5 | 86.4 | 0.0 | 20.2 | 30.5 | 11.2 | 13.3 |
| **Hubnerite** | 0.0 | 0.8 | 0.1 | 0.0 | 0.0 | 0.0 | 0.0 |
| **Cassiterite** | 0.2 | 0.2 | 0.4 | 0.0 | 0.0 | 0.2 | 0.5 |
| **Fe Oxide** | 60.9 | 2.9 | 19.7 | 0.9 | 25.0 | 0.0 | 43.3 |
| **Quartz** | 2.2 | 0.4 | 1.5 | 0.0 | 4.2 | 2.8 | 0.0 |

The potential for gravity separation can be illustrated by dividing particles analysed by QEMSCAN into size and density categories. This was achieved by importing data from false colour images generated by QEMSCAN in to Mathworks Matlab 2017b. Within the software, the diameter of each particle was calculated as the minor axis of the ellipse that had the same normalized second central

moment as the particle. The density of particles was calculated as a weighted average of the minerals distributed within the particle; where mineral densities were taken as standard mineral values. Some caution needs to be used when interpreting these data as the density of the weathered minerals is not standard and it is difficult to measure directly. Densities were estimated for these mineral categories using a linear interpolation based on the average proportion of tungsten in the mineral structure and the standard densities of ferberite and hematite. The particles were then classified into size and density categories. Figure 9 shows the mass distribution in the size and density categories generated.

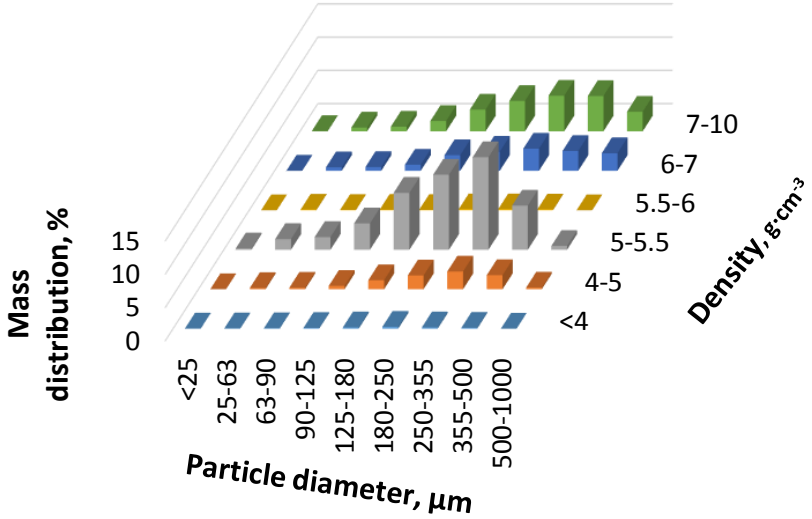


**Figure 9.** Mass distribution of particles in size and density categories generated using Mathworks Matlab 2017b.

In Figure 9 there are two distinct peaks at S.G. 5–5.5 and S.G. 6–10. This can be interpreted as the relatively liberated hematite and wolframite series minerals. The concentration criterion for this separation (Equation (3)) is 1.4, based on an average particle density in the S.G. 5–5.5 range of S.G. 5.28 and in the S.G. 6–10 ranges of S.G. 6.98 and assuming the fluid density to be S.G. 1.00.

$$concentration\ criterion = \left( \frac{\rho_{heavy} - \rho_{fluid}}{\rho_{light} - \rho_{fluid}} \right) \quad (3)$$

This value would suggest that the separation is very difficult [17] which agrees well with the prior knowledge of the material and in fact shows that the task is more difficult than initially anticipated as the concentration criterion for a separation of un-weathered ferberite from hematite is 1.5. This suggests that a centrifugal separator is likely to be required and that MGS would be a good candidate.

### *3.2. Particle Size Analysis*

The size distribution of the stage ground material is reported in Figure 10. The size analysis was undertaken on completion of the test programme. The $P_{80}$ of the material was 61 µm with 10% less than 4 µm.

The particle size distribution of the material is in a suitable range for efficient separation by MGS. There is a significant proportion of minus 10 µm material which would be expected to adversely affect the separation.

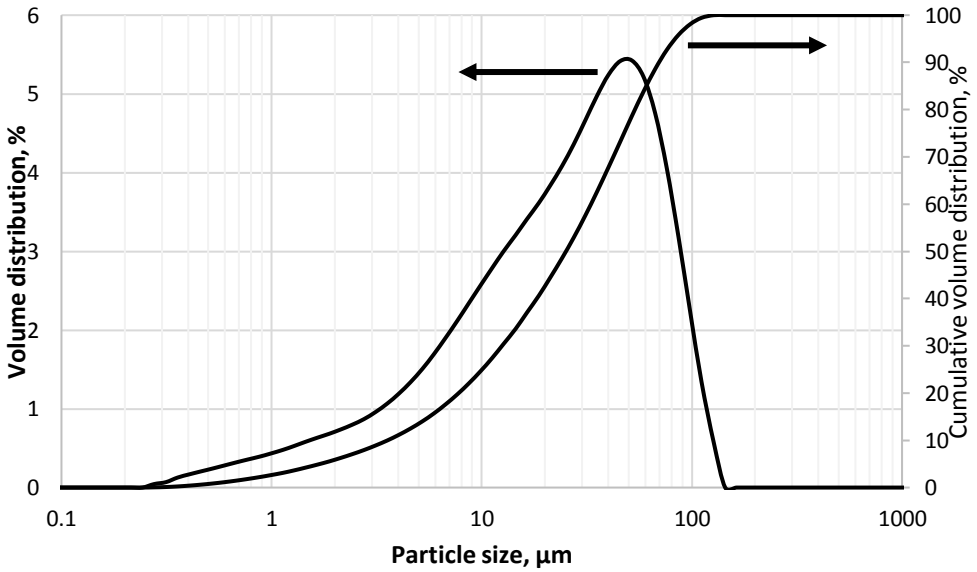


**Figure 10.** Size distribution of feed material for testwork as measured by a Malvern Mastersizer 3000 laser diffractometer. Particle size is reported as equivalent spherical diameter.

### *3.3. Selective Concentration by Enhanced Gravity Concentrator*

#### 3.3.1. Experimental Results

The results of the initial test work to determine the time required to reach a steady state and consequently appropriate sampling times to ensure representative samples. Experiments were undertaken sequentially and so it was necessary to determine the time required to reach steady state on machine start-up and after changes to feed conditions. The results of these experiments are summarised in Figures 11 and 12.

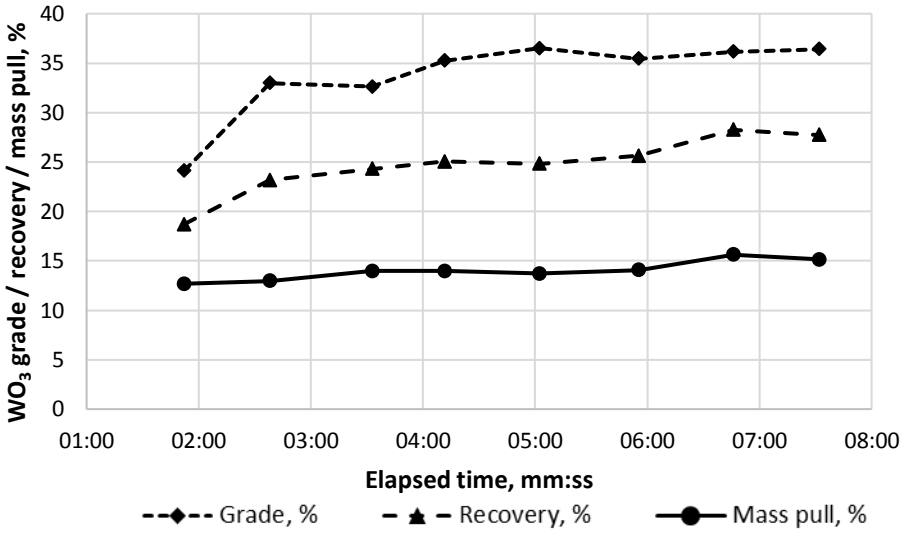


**Figure 11.** Results of experiments to monitor variation in concentrate grade, recovery and mass pull to concentrate outlet over time.

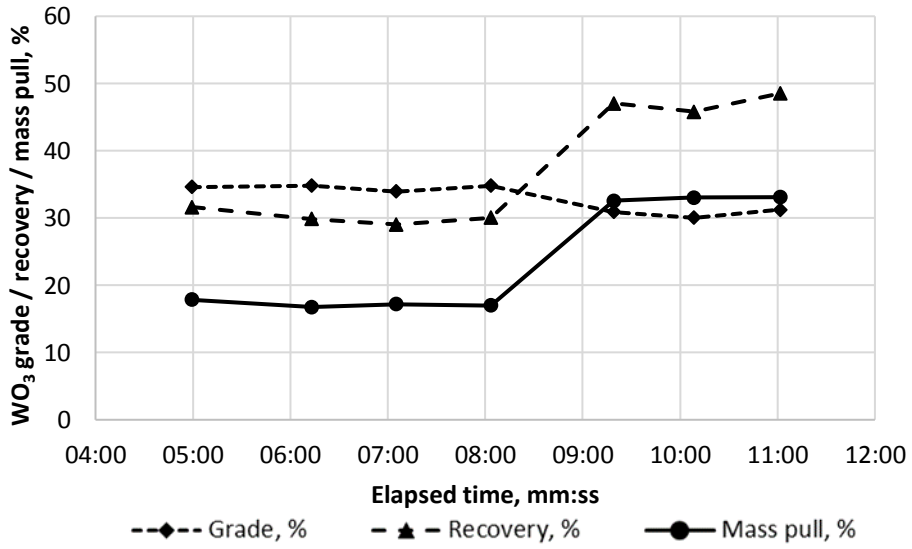


**Figure 12.** Results of experiments monitoring variation in concentrate grade, recovery and mass pull to concentrate outlet over time when changing wash water flowrate.

Figure 11 shows that a steady state is reached after about 4–5 min from machine start-up. Figure 12 shows that after further changes to wash water a steady state is reached after about 1–2 min. Due to limitations in the mass of feed material available it was not possible to run beyond 11 min at the tested solid feed rate. Based on the above results, for each run of the experimental design, samples were collected at 6 min and 7 min after setting the desired conditions.

Figure 13 shows the grade-recovery curve for the experiments undertaken as a part of the CCRD design. The figure shows that the maximum recovery above the required grade of 43% $WO_3$ was approximately 31%.

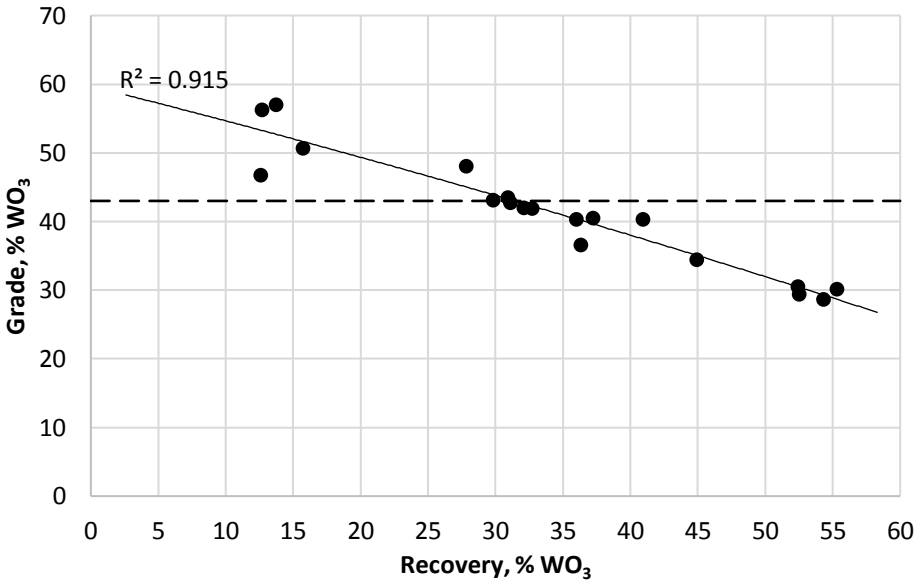


**Figure 13.** Grade-recovery curve for experimental runs. The dashed line indicates the minimum required $WO_3$ grade set by the mine operator and the solid line is a 2-degree polynomial line of best fit with $R^2$ value of 0.915.

The MGS was then modelled with the experimental results using the response surface methodology within Minitab 17. The resultant equation linking the input variables to recovery

and grade are shown in Equations (4) and (5). The response surfaces generated are shown in Figures 14 and 15.

$$\begin{aligned}\text{Recovery} = \; & -2515 + 33.6 \cdot x_1 + 34.0 \cdot x_2 - 4.52 \cdot x_3 - 0.1102 \cdot x_1 \cdot x_1 + 0.727 \cdot x_2 \cdot x_2 \\ & - 0.0394 \cdot x_3 \cdot x_3 - 0.349 \cdot x_1 \cdot x_2 + 0.0485 \cdot x_1 \cdot x_3 + 0.140 \cdot x_2 \cdot x_3\end{aligned} \tag{4}$$

$$\begin{aligned}\text{Grade} = \; & 1095 - 13.42 \cdot x_1 + 13.5 \cdot x_2 - 1.68 \cdot x_3 + 0.0420 \cdot x_1 \cdot x_1 - 0.351 \cdot x_2 \cdot x_2 \\ & + 0.0087 \cdot x_3 \cdot x_3 - 0.0606 \cdot x_1 \cdot x_2 + 0.0063 \cdot x_1 \cdot x_3 + 0.0249 \cdot x_2 \cdot x_3\end{aligned} \tag{5}$$

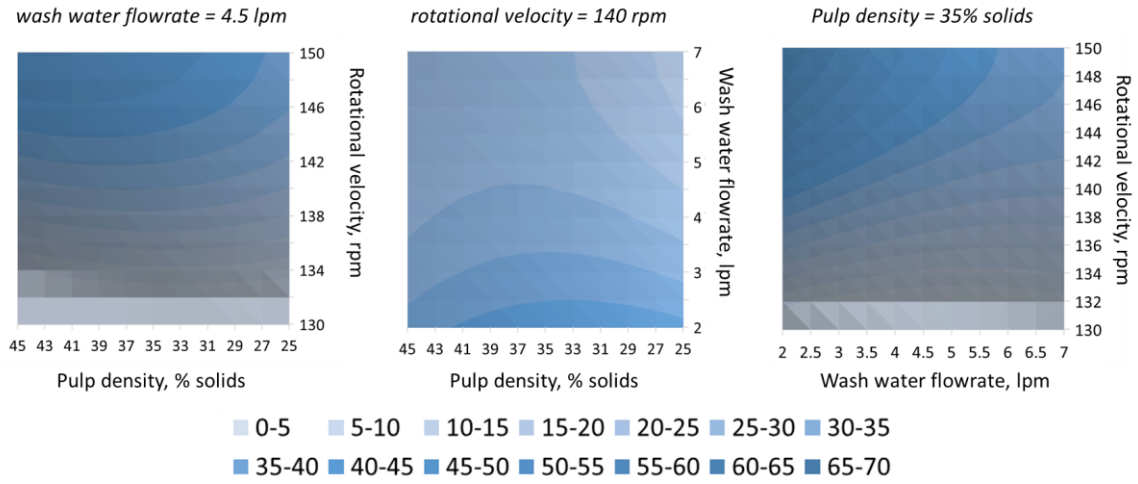


**Figure 14.** Response surface plots of $WO_3$ recovery to MGS concentrate stream at fixed variable positions.

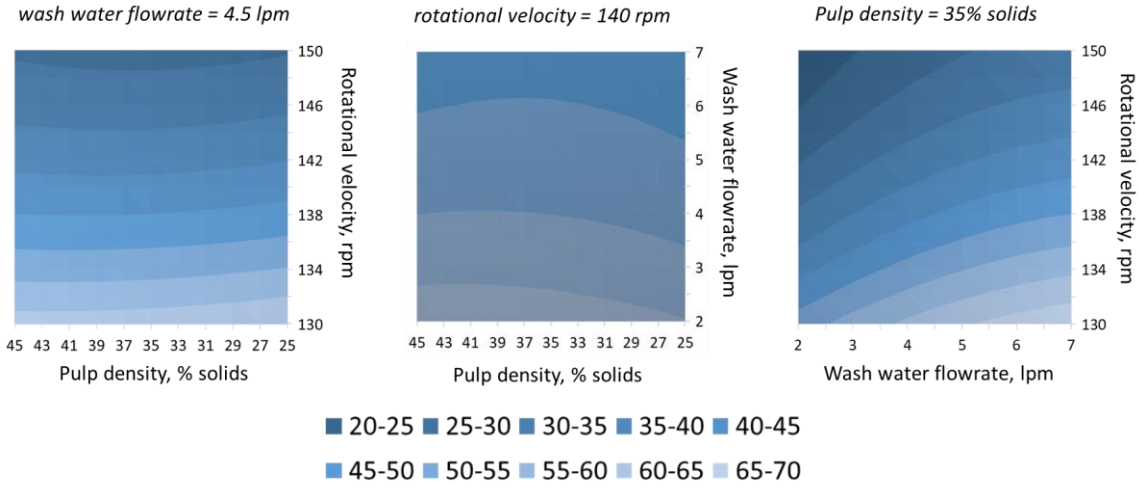


**Figure 15.** Response surface plots of $WO_3$ grade in the MGS concentrate stream at fixed variable positions.

The graphs for recovery presented in Figure 14 show an increasing recovery with increasing rotational velocity ($x_1$) and decreasing wash water flowrate ($x_2$). The pulp density ($x_3$) has a positive effect on recovery between 36–38% solids with a decrease in recovery the further from this density the slurry becomes. The recovery graphs also suggest that at high wash water levels an increase on % solids in the slurry will add to recovery. The graphs for the grade model presented in Figure 15 show that grade increases with decreasing rotational velocity. Increasing wash water flowrate and pulp density have very little effect on the produced grade.

Using ANOVA, it was found that the rotational velocity had the most effect on recovery followed by wash water flowrate with these two variables also having the strongest interaction effect. The importance of rotational velocity agrees well with the literature. However, the importance of wash water was more than that of pulp density which is contrary to [6,8]. The strong interaction effect between rotational velocity and wash water is in agreement with [9].

### 3.3.2. Validation of Results

To test the validity of the generated model it was examined using a number of statistical measures. Firstly, the experimental errors were measured. It was found that the standard deviation for $WO_3$ grade for the repeated central point experimental runs was 1.4%. For the recovery the standard deviation was 4.2%. This error is a combination of the analytical error and errors in obtaining the same pulp density and feed rate between test runs. The standard deviation between repeat analytical readings was 0.6% $WO_3$, suggesting that most of the error was due to inaccuracy in experimentation.

To ensure that there were no significant variations in feed grade during the experimental runs, which would mask the effects of operating variables, the calculated feed grade was plotted against experimental run date (Figure 16).

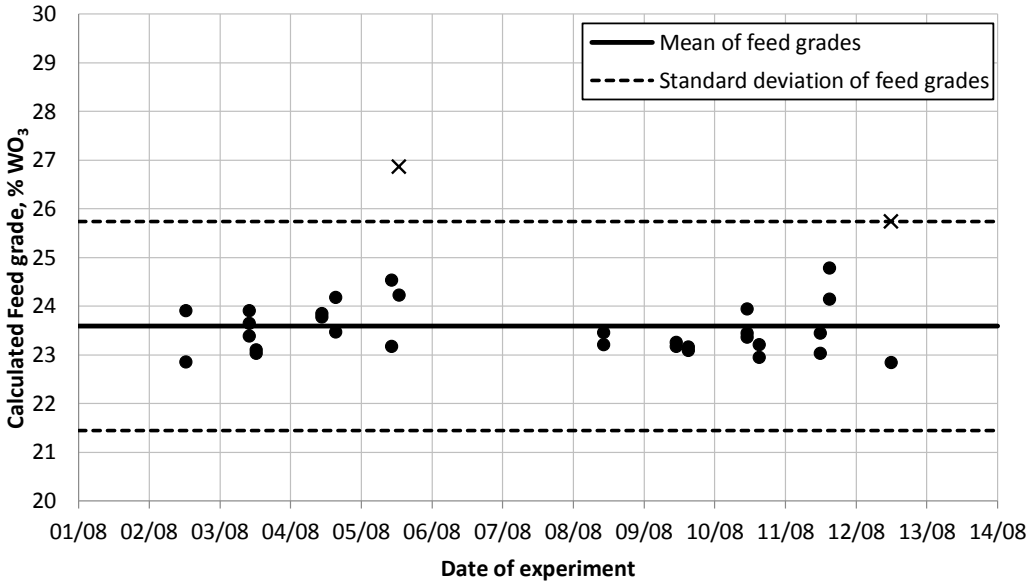


**Figure 16.** Variation in $WO_3$ feed grade over all experimental runs. X denotes outliers removed from the dataset.

The chart shows that most data points fit within the average standard deviation of analytical error (±0.6%) with two outliers identified and removed. For the test runs containing outliers, results are based on a single sample not an average of both samples. There is no discernible trend in the feed grade over the course of the experimentation which suggests a lack of bias over time. This also indicates that the loss of fines during the test programme was minimal.

The fit of the models generated using the Response Surface Method can be assessed using the adjusted $R^2$ values (Table 5).

**Table 5.** Adjusted $R^2$ values for fitted models of grade and recovery.

| Model | Adjusted $R^2$ Measure of Fit |
|---|---|
| $WO_3$ Grade | 95.4% |
| Recovery | 91.5% |

Table 5 shows that the models account for most of the variation in the grade and recovery. The grade model is better fitted to the data which is not unexpected due to the lower measured experimental error. Model fits showed that most points fit within the 95% confidence interval for the mean response and all fall within the 95% confidence interval for predicting values.

### 3.3.3. Comparison to Conventional Scraping Blades

To assess the influence of the novel low profile scraping blades, suitable data points for comparison were taken from a dataset of results for both conventional and low profile scraping blades. The dataset for conventional blades was formed from test work undertaken both before and after the CCRD-RSM experimental programme. The tests undertaken using conventional blades represent a range of test conditions with the wash water flow rate, pulp density and drum velocity varied to obtain a range of values. The dataset for the low profile scraping blades combined the results of the CCRD-RSM experiments with further tests undertaken afterwards. Suitable data points for comparison were selected based on equivalence in $WO_3$ feed grade and stability of mass flow rate to ensure the validity of the comparison. This was important as it was found that the residence time for concentrate material using the conventional scraping blades was longer than for the low profile blades and it was not possible in all tests to reach a steady state due to limitations in the feed available. This tended to result in lower reported feed grades or mass flow rates. There was a slight trend towards lower feed grades in later test-work. This is expected to be a result of general loss of material during testing (spillages, etc.) which reduced the feed mass and so maximum experiment run time but also due to some degradation of the ferberite over time. Further QEMSCAN analyses would allow for better understanding of this issue but this was not undertaken as a part of the study.

The methodology used to select valid data points was to firstly reject tests in which the measured mass flow rate was less than 85% of the or where the feed grade was less than 20% $WO_3$. The average feed grade of the data remaining in the conventional scraping blade dataset was then calculated and data points from both datasets rejected where the relative difference to this average value was greater than 2 standard deviations (1.65%). In total 20 data points were rejected and 21 data points accepted. From the dataset of conventional scraping blade tests accepted, 7 tests were completed before the CCRD-RSM experimentation programme and 1 test afterwards.

Figure 17 shows the $WO_3$ grade recovery curve for the accepted data points valid for comparison.

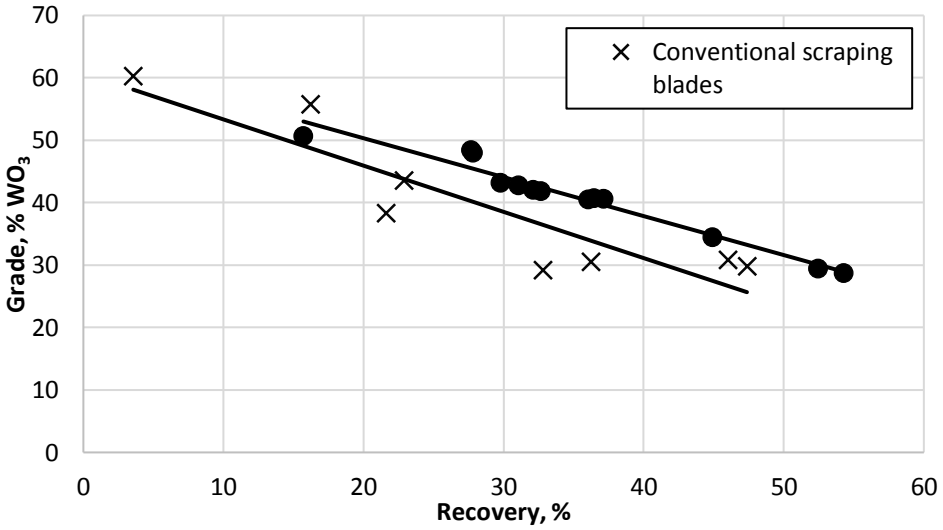


**Figure 17.** Grade-recovery plot for comparable data points of low profile and conventional scraping blade tests. The solid lines indicate the fitted regression lines.

Analysis of co-variance (ANCOVA) was undertaken using Mathworks Matlab 2017b to determine if there was a statistically significant difference in the regression lines for the two datasets of comparable data points. The results of this analysis indicated that the difference in the slope of the two regression lines was not significant at 95% confidence level ($p$-value = 0.47). The difference between the regression lines was significant ($p$-value = 0.002) at a 95% confidence level.

Further comparison was drawn by creating enrichment ratio-recovery curves for data points within 2 standard deviations and 3 standard deviations. Where the enrichment ratio is taken as the ratio of concentrate grade to feed grade. These comparisons are summarised in Figure 18.

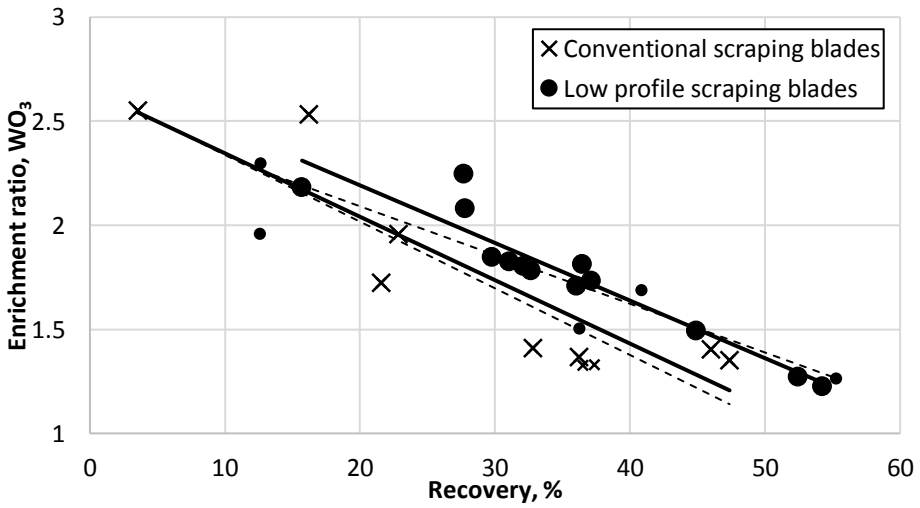


**Figure 18.** Enrichment ratio-recovery plot for comparable data points of low profile and conventional scraping blade tests. The solid lines indicate the fitted regression lines for points within 2 standard deviations of the mean. The dotted lines indicate the fitted regression lines for the points within 3 standard deviations.

Figure 18 shows that when differences in feed grade are accounted using an enrichment ratio the low profile scraping blades shows improved performance of conventional blades for the tests compared. For points within 2 and 3 standard deviations there was not sufficient statistical evidence that the regression lines slopes were different at the 95% level but there was sufficient evidence that the low profile blades made a difference to performance. However, at a 90% level there was sufficient evidence of different slopes for data points within 3 standard deviations. This can be seen in Figure 18 at low recoveries where the upgrade using conventional scraping blades may perform better than for the low profile blades.

Further experimentation is required to investigate this improvement to increase statistical reliability and ensure optimal conditions for the conventional blades. Further, the applicability of the result to other materials must be tested. With these caveats, it can be said that the results show that the low-profile blades offer significant potential and merit further investigation to optimise the design. Further experimentation was not possible in this instance due to insufficient material remaining to reach steady state using conventional blades, potentially compounded by degradation of the material.

## 4. Conclusions

The results of the test work using a Mozley MGS with novel scraping blades has been reported. The LIMS magnetic fraction used for testing contained valuable, liberated ferberite indicating the potential for recovery by physical separation. QEMSCAN data showed that the ferberite in the stream was weathered and depleted in tungsten and that the main gangue mineral was hematite, limiting the options for equipment to separate the material. The Mozley MGS is well suited for this type of separation.

Using the response surface methodology with CCRD design it was possible to model the grade and recovery of $WO_3$ when varying the rotational velocity, wash water flow rate and feed pulp density. The models generated by RSM fitted the data well with adjusted $R^2$ of 95.4% and 91.5% for the grade and recovery of $WO_3$, respectively. This indicated that the variables selected accounted for over 90% of the observed variation in results. Of the remaining variability in each model approximately half was a result of experimental errors.

Test work showed that it was possible to recover ferberite from the LIMS stream which meets the required minimum grade. The maximum reported recovery which met the required grade was 32.7%. Although relatively low, the tungsten recovered would otherwise be lost as waste. Comparison of the new blades with traditional ones indicate that for this material there was a significant improvement in separation performance in the region of the required minimum grade. Further experimentation is required to investigate this improvement but the results indicate that the low-profile blades offer significant potential and merit further investigation to optimise the design.

**Author Contributions:** R.F. and K.F. conceived and designed the experiments; K.F., P.H., T.M. performed the experiments; R.F., P.H., G.R. and W.X. analyzed the data; G.R. and P.H. contributed analysis tools; T.M. contributed prototype low profile blades; R.F. wrote the paper with contributions from K.F and G.R.

**Acknowledgments:** This work is part of the OptimOre project. This project has received funding from the European Union's Horizon 2020 research and innovation programme under grant agreement No. 642201. Authors are thankful to Wolf Minerals for providing material for experimentation and to Gravity Mining Ltd. for support in undertaking experiments and providing the opportunity to test the modified low profile blades.

**Conflicts of Interest:** The authors declare no conflict of interest.

## References

1. European Commission. *Study on the Review of the List of Critical Raw Materials*; European Commission: Brussels, Belgium, 2017; pp. 33–35.
2. European Commission. *Report on Critical Raw Materials for the EU—Critical Raw Materials Profiles*; European Commission: Brussels, Belgium, 2015; pp. 193–202.
3. Chan, B.S.K.; Mozley, R.H.; Childs, G.J.C. Extended trials with the high tonnage multi-gravity separator. *Miner. Eng.* **1991**, *4*, 489–496. [CrossRef]
4. Glass, H.J. Separating small particles with the multi-gravity separator. In *Innovation in Physical Separation Technologies: Richard Mozley Memorial Volume. Papers Presented at the "Innovation in Physical Separation Technologies" Conference*; IMM: London, UK, 1998; pp. 161–171. ISBN 978-1-870706-33-9.
5. Ahmadabadi, A.D.; Hejazi, R.; Saghaeian, S.M. Statistical evaluation and optimization of multi-gravity separator (MGS) parameters for upgrading of chadormalu ultra-fine haematite tailings. In Proceedings of the International Mineral Processing Congress—IMPC 2012, New Delhi, India, 23–28 September 2012; pp. 2016–2025.
6. Aslan, N. Application of response surface methodology and central composite rotatable design for modeling the influence of some operating variables of a Multi-Gravity Separator for coal cleaning. *Fuel* **2007**, *86*, 769–776. [CrossRef]
7. Turner, J.W.G.; Hallewell, M.P. Process improvements for fine cassiterite recovery at Wheal Jane. *Miner. Eng.* **1993**, *6*, 817–829. [CrossRef]
8. Venkateswara, G.; Sharma, S.K.; Markandeya, R. Modeling and optimization of Multigravity separator for recovery of Iron values from Sub Grade Iron Ore. In Proceedings of the International Mineral Processing Congress—IMPC 2014, Santiago, Chile, 20–24 October 2014.
9. Aslan, N. Application of response surface methodology and central composite rotatable design for modeling and optimization of a multi-gravity separator for chromite concentration. *Powder Technol.* **2008**, *185*, 80–86. [CrossRef]
10. Chaurasia, R.C.; Nikkam, S. Optimization Studies on a Multi-Gravity Separator Treating Ultrafine Coal. *Int. J. Coal Prep. Util.* **2017**, *37*, 195–212. [CrossRef]

11. Ozgen, S. Modelling and optimization of clean chromite production from fine chromite tailings by a combination of multigravity separator and hydrocyclone. *J. South. Afr. Inst. Min. Metall.* **2012**, *112*, 387–394.
12. Rao, G.V.; Markandeya, R.; Sharma, S.K. Process amenability studies of sub grade iron ore from Bacheli complex, Bailadila sector, India. In Proceedings of the International Mineral Processing Congress—IMPC 2012, New Delhi, India, 23–28 September 2012; pp. 1840–1860.
13. Pascoe, R.D.; Power, M.R.; Simpson, B. QEMSCAN analysis as a tool for improved understanding of gravity separator performance. *Miner. Eng.* **2007**, *20*, 487–495. [CrossRef]
14. Obeng, D.P.; Morrell, S.; Napier-Munn, T.J. Application of central composite rotatable design to modelling the effect of some operating variables on the performance of the three-product cyclone. *Int. J. Miner. Process.* **2005**, *76*, 181–192. [CrossRef]
15. Napier-Munn, T.J. *Statisitcal Methods for Mineral Engineers—How to Design Experiments and Analyse Data*; Julius Kruttschnitt Mineral Research Centre: Indooroopilly, QLD, Australia, 2014, ISBN 978-0-9803622-4-4.
16. Keats, W. Alteration and Replacement of Wolframite in the Hemerdon Tungsten Deposit, Devon. Ph.D. Thesis, Camborne School of Mines, Camborne, UK, 1981.
17. Wills, B.A.; Finch, J. *Wills' Mineral Processing Technology, Eighth Edition: An Introduction to the Practical Aspects of Ore Treatment and Mineral Recovery*, 8th ed.; Butterworth-Heinemann: Oxford, UK, 2015, ISBN 978-0-08-097053-0.